Ontogenetic plasticity in cranial morphology is associated with a functional change in the food processing behavior in Alpine newts

Daniel Schwarz[1]*, Nicolai Konow[2], Laura B. Porro[3], Egon Heiss[1]

Abstract

Background: Salamander morphology changes substantially during metamorphosis, prompting the hypothesis that larvae need a different processing mechanism than post-metamorphic adults. Salamandrid newts with facultative metamorphosis are suitable for testing this hypothesis, because paedomorphic and metamorphic adults often coexist in the same population. Facultative paedomorphic newts provide a direct comparison of form-function relationships with specimens of the same species sharing similar body size and feeding on overlapping prey spectra, whilst having divergent food-processing morphologies.

Methods: We use high-speed videography to quantify the *in vivo* movements of key anatomical elements during food processing in paedomorphic and metamorphic Alpine newts (*Ichthyosaura alpestris*). Additionally, we use micro-computed tomography (µCT) to analyze morphological differences in the feeding apparatus of paedomorphic and metamorphic Alpine newts and sort them into late-larval, mid-metamorphic and post-metamorphic morphotypes.

Results: Paedomorphic and metamorphic individuals exhibited clear morphological differences of their feeding apparatus. Regardless of the paedomorphic state being externally evident, different paedomorphic specimens can conceal different morphotypes (i.e., late-larval and mid-metamorphic morphotypes). Though feeding on the same prey under the same (aquatic) condition, food processing kinematics differed between late-larval, mid-metamorphic and post-metamorphic morphotypes.

Conclusions:

While the Alpine Newt still lives in water, food processing mechanism changes along with morphology of the feeding apparatus during ontogeny, from a mandible-based to a tongue-based processing mechanism as the mandible's changing morphology prevents chewing and the tongue allows enhanced protraction. These results could indicate that early tetrapods, in analogy to salamanders, may have developed new feeding mechanisms in their aquatic environment and that these functional innovations may have later paved the way for terrestrial feeding mechanisms.

Keywords: Chewing, feeding, kinematics, micro-CT, high-speed videography, salamander, morphology, food-processing apparatus, ontogeny, intraoral food processing

* Correspondence: Daniel.schwarz@uni-jena.de

[1]Institute of Zoology and Evolutionary Research, Friedrich-Schiller-University Jena, Erbertstraße 1, D-07743 Jena, Germany; [2]Department of Biological Sciences, University of Massachusetts Lowell, 198 Riverside St., Lowell, MA 01854, USA.; [3]Centre for Integrative Anatomy, Department of Cell and Developmental Biology, University College London, London, WC1E 6BT, UK.

Background

Most salamanders switch from a 'free-feeding' larval- to a post-metamorphic stage during ontogeny via metamorphosis [1–3]. However, some salamanders do not undergo metamorphosis but instead attain sexual maturity while retaining larval traits [4,5]. This somatic developmental arrest is referred to as paedomorphosis, and is particularly common among salamanders [6–9]. In some salamander species, individuals can either undergo or skip metamorphosis (i.e., facultative paedomorphosis) [7,10], resulting in paedomorphic and metamorphosed adults co-populating similar niches of a habitat whilst differing in morphology (i.e., heterochronic morphotypes). Prior studies have hypothesized that, due to their different morphologies, heterochronic morphotypes differ in their feeding performance (capture success-rate) and feeding behavior [11–13]. Behavioral studies have shown that paedomorphs tend to have greater aquatic prey capture performance [11,13], but surprisingly, despite diverging prey capture performance and major differences in head morphology, there are only minor differences in prey capture kinematics between heterochronic morphotypes [12–15].

Prey capture is followed by intraoral behaviors, which can include distinct processing and transport cycles. Similar to prey capture kinematics, transport kinematics do not seem to differ significantly between aquatic and terrestrial morphotypes [16–19]. However, it is unclear whether intraoral processing kinematics follow the same pattern as capture and transport. First, although recent evidence suggests that intraoral food processing is more common in salamanders than previously thought [20–22], processing remains little studied in salamanders compared to other taxa [23,24]. Second, processing might be affected more from differing feeding apparatus morphologies than capture and transport. This latter possibility becomes more evident if we consider changes in: the structure, position and number of the teeth [25–28]; structural changes of the hyobranchial apparatus (i.e., developing from a gill-bearing to a tongue-bearing apparatus) [13,14,29–31]; changes in the muscular and ligamentous suspension of the hyobranchial apparatus [32–34]; morphological changes of mandible and skull [14,35–37]; as well as dramatic muscular reorganization [38,39] during metamorphosis in salamanders. All of the aforementioned characteristics impact intraoral food processing kinematics in salamanders [20,22].

Food processing in salamanders involves a mix of structural and functional traits seen in fishes and amniotes [20]. Salamanders, being lissamphibians, are especially interesting from an evolutionary point of view because of their phylogenetic position near the base of the tetrapod radiation, with lissamphibians being considered the extant sister-group of amniotes. As a result, salamanders are critical to our understanding of the functional evolution of tetrapods, because they might retain many basal features in the musculoskeletal system [40,41], including a broad and flat skull [42,43], and a similarly robust anatomy of the hyobranchial apparatus [44]. The lissamphibian metamorphosis enables the experimental investigation of developmental water-land transitions in recent tetrapods [40] – as an analogy to the evolutionary water-land transitions of early tetrapods.

Accordingly, our objectives in the present study are: a) to compare the intraoral food processing kinematics and feeding apparatus morphologies of the heterochronic morphotypes of the Alpine newt (*Ichthyosaura alpestris*) and b) to propose a possible evolutionary scenario of the prey-processing behavior in early tetrapods. We quantify how changes in form of the feeding apparatus can induce shifts in feeding kinematics. We hypothesize that while prey capture and transport kinematics are similar between paedomorphic and metamorphic Alpine newts, intraoral processing kinematics will differ between heterochronic morphotypes.

Results

Functional morphology of the food-processing apparatus

Detailed descriptions of the cranial anatomy of *Ichthyosaura alpestris* and other salamandrids can be found elsewhere [25,31,45–51] and we focus on structures relevant for processing and on specific differences between morphotypes.

Cranial osteology

The feeding apparatus of the Alpine newt consists of an osseous skull and mandible, and a complex, partially cartilaginous hyobranchial system (i.e., hyobranchial in larval or hyolingual in metamorphosed salamanders, respectively) (see Fig. 1) and prominent muscles (Fig. 2). We group the specimens into three distinct morphotypes: (i) late-larval, (ii) mid-metamorphic, and (iii) post-metamorphic based on their developmental state. The anterior skull plates of the late-larval morphotype (LLM) are largely unfused while in the mid-metamorphic morphotype (MMM) and the post-metamorphic morphotype (PMM) the enlarged frontal bones fill those gaps. The pterygoids of LLM and MMM are relatively small compared to those of the PMM. All morphotypes carry two functional upper jaw systems: the first consists of the tooth bearing maxilla and premaxilla (i.e., primary upper jaw), and the second of the tooth bearing vomerine and palatine bones of the mouth roof (i.e., secondary upper jaw or palatal jaw).

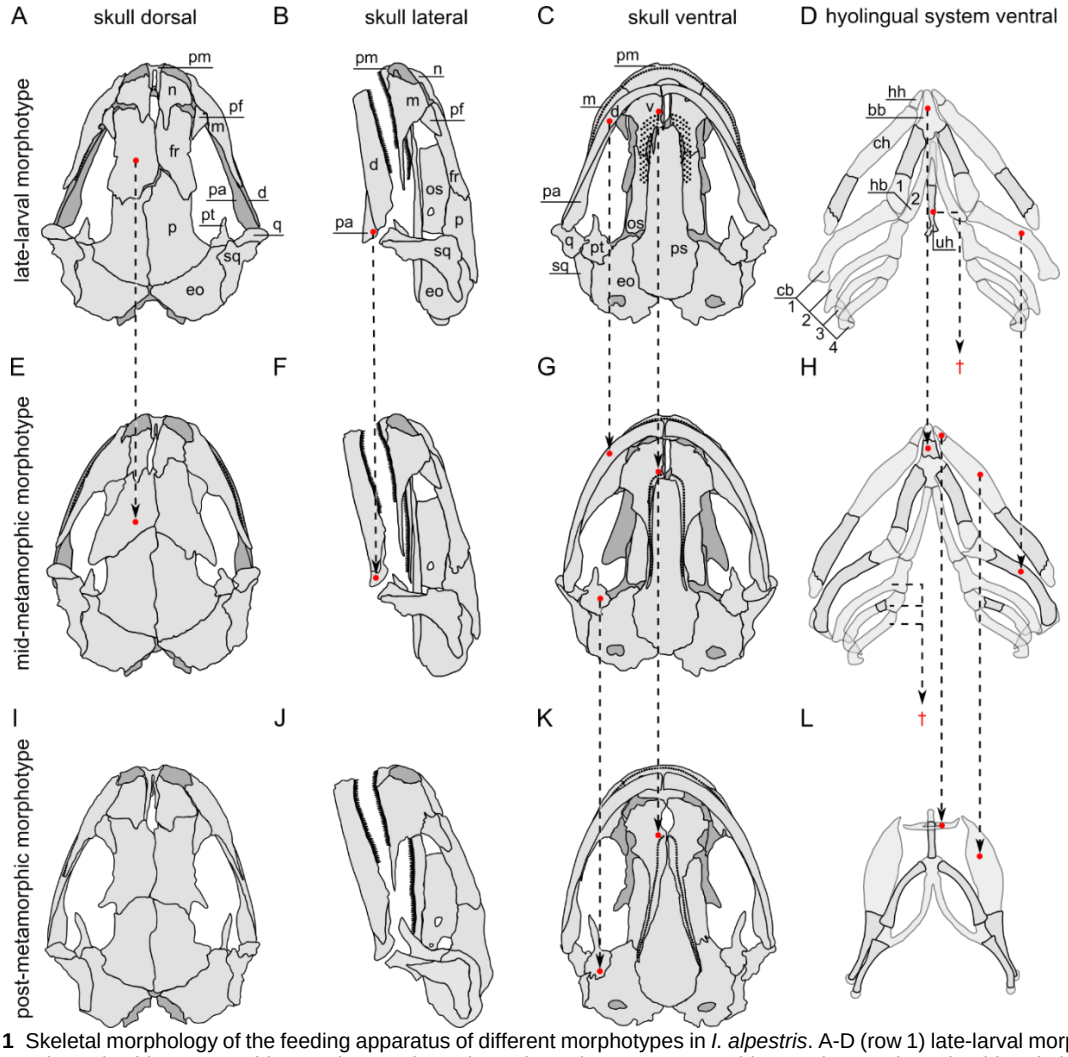

Figure 1 Skeletal morphology of the feeding apparatus of different morphotypes in *I. alpestris*. A-D (row 1) late-larval morphotype (LLM), E-H (row 2) mid-metamorphic morphotype (MMM), I-L (row 3) post-metamorphic morphotype (PMM). Abbreviations: bb,

basibranchial; cb 1 - 4, ceratobranchial 1 - 4; ch, ceratohyal; d, dentary; eo, exoccipital; fr, frontal; hh, hypohyal (also referred to as radial); hb 1 - 2, hypobranchial 1 - 2; m, maxilla; n, nasal; os, orbitosphenoid; p, parietal; pa, prearticular; pf, prefrontal; pm, premaxilla; ps, parasphenoid; pt, pterygoid; q, quadrate; sq, squamosal; uh, urohyal; v, vomer. Arrows connecting different morphotypes (rows) highlight significant structural differences. Arrows ending in the space between morphotypes marked with † indicate the reduction of the structure.

The palatal dentition pattern of the LLM is U-shaped and the teeth organized in rows, the mandible is slightly V-shaped in ventral view and the functional occlusal surface for the lower jaw dentition is the palate between primary and secondary upper jaws. The mandibles of MMM and PMM are U-shaped in ventral view and the occlusal surface for the lower jaw are the maxillary teeth of the primary upper jaw. The palatal dentition of the MMM and the PMM are distinct as the MMM has a U-shaped single row of denticles and the PMM exhibits a V-shaped single row of denticles.

Hyobranchial musculoskeletal anatomy

The hyobranchial apparatus shows the most striking differences between morphotypes. In the LLM, the hyobranchial apparatus is a complex and mainly cartilaginous system with small ossification centers in ceratohyal, hypobranchial and urohyal. The hyobranchial apparatus of MMM shows enlargement of these ossified centers, additional ossification centers in basibranchial, ceratobranchial 1 and 3, as well as the reduction of the urohyal. The hyolingual apparatus of the PMM exhibits a typical morphology for metamorphosed salamandrids. Thus, in the PMM the ceratobranchial 2 - 4 are reduced and the hypohyals merge to form a buckle around basibranchial (often referred to as the radial).

Our functional descriptions of the hyobranchial apparatus focus on muscles responsible for the main movements of the anterior tip of the hyobranchial system (i.e., the basibranchial). The 3D muscle morphology is considered but the main function of each muscle is assessed from a lateral perspective (i.e., simplified to a 2D movement). More complex inter-hyobranchial movements are likely to occur due to the 3D orientation of the hyobranchial apparatus and its muscles (see for example [52]). The hyobranchial system of all morphotypes forms the attachment site for several major muscles (i.e., six in the LLM and MMM, and five in the PMM). The muscles can be differentiated according to their initial attachment to hyoid arch or branchial arch during ontogeny [53]. The hyoid arch (paired ceratohyals) is connected with the hyomandibular (HM) muscle in the PMM, and also with the levator hyoideus (LH) in the LLM and MMM. The HM runs between the ossified area of the ceratohyal and the dentary in all morphotypes, acting as a protractor of the hyobranchial system. In the LLM, the LH originates on the dorsal squamosal process and attaches to the upper osseous part of the ceratohyal, while in the MMM the LH originates from the mid-squamosal and attaches to the upper osseous part of ceratohyal. Accordingly, the LH serves as a hyobranchial elevator in LLM and MMM. The LH is missing in the PMM because the LH detaches from the hyobranchial system during development in order to attach to the lower jaw and thus form the depressor mandibulae posterior. Apart from the development of the depressor mandibulae posterior, the cranial muscles for opening and closing the jaw showed no significant differences between the morphotypes. The branchial arch is connected with geniohyoid (GH), branchiohyoideus externus (BHE), subarcualis rectus 1 (SR1), and rectus cervicis (RC). The thin GH muscle runs from the basibranchial to the dentary in all morphotypes, thus enabling protraction of the hyobranchial system. A peculiarity in metamorphs is that some fibers of the GH run from the pericardium to the dentary [46]. The fleshy BHE extends from the lateral side of the postero-dorsal ceratobranchial I to the antero-lateral side of the osseous hypobranchial I in the LLM. Thus, the BHE bends the articulation between hypobranchial 1 and ceratobranchial 1, and serves as an elevator of the anterior part of the

branchial system. In contrast, in the MMM and the PMM, the insertion of the BHE shifted to the antero-ventral part of ceratohyal and therefore acts as a protractor of the branchial arch. The SR1 extends from the antero-ventral side of the cartilaginous ceratobranchial I to the medio-lateral region of the hypobranchial I in the LLM, acting as antagonist of the BHE by depressing the tip of the hyobranchial system, while in the MMM and the PMM the SR1 extends from the medial part of the ceratobranchial I to the medio-lateral part of the ceratohyal to act as a protractor of the branchial arch. The most prominent muscle of the hyobranchial system in all morphotypes is the RC that originates from the ventral abdominal trunk muscles and inserts onto the basibranchial. Due to its course and the ligament and muscle suspension of the hyobranchial apparatus on the skull (hyomandibular or hyoquadrate ligament and levator hyoideus), the RC facilitates retraction and depression of the hyobranchial apparatus.

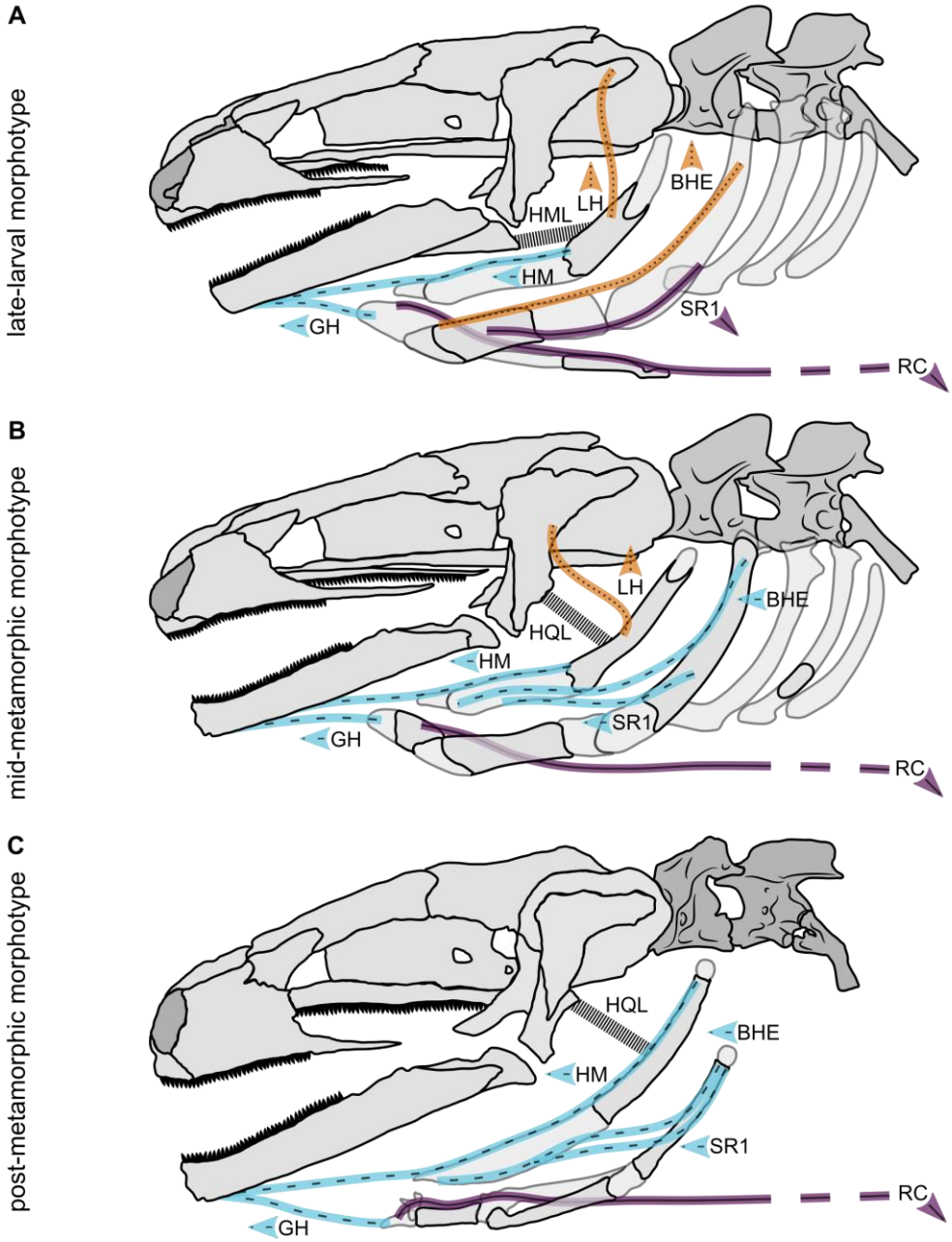

Figure 2 Muscular morphology of the feeding apparatus of three different morphotypes of *I. alpestris*: (A) the late-larval morphotype (LLM), (B) the mid-metamorphic morphotype (MMM), (C) the post-metamorphic morphotype (PMM). Muscles: (BHE) branchiohyoideus externus, (GH) geniohyoideus, (HM) hyomandibularis, (LH) levator hyoideus, (RC) rectus cervicis and (SR1) subarcualis rectus 1. Ligaments: hyomandibular ligament (HML) and hyoquadrate ligament (HQL). The directional effect of each muscle on the movement of the tip of the hyobranchial apparatus (i.e., the basibranchial) is encoded by the arrows, protractors (blue and dashed), retractors and depressors (purple and solid), and elevators (orange and dotted). Note that there is no direct

hyobranchial elevator in the PMM. Depression of the hyobranchial system is achieved by a combination of rectus cervices activity and the ligamentous and muscular suspension of the hyobranchial skeleton to the skull. Please note that the course of the ligaments was obtained from other morphological descriptions [32,34,47] and could not be verified in this study.

Intraoral food processing

After initial ingestion via suction feeding, one or two transport movements were used by all morphs to position prey prior to a consecutive set of processing cycles. The mean total processing cycles were 5.7 ± 3.2 (mean ± S.D.) for the larval, 5.6 ± 2.4 for the mid-metamorphic, and 5.9 ± 2.5 for the post-metamorphic morphotypes. A processing cycle was defined from start of gape opening until the next start of gape opening. Processing involved the cyclical opening and closing of the jaw (i.e., arcuate mandible movement), elevation and depression of the hyobranchial apparatus (i.e., the tongue) and, in the metamorphic morphotype only, additional rhythmic flexion and extension of the neck (vertical cranial movement) (Fig. 3 C). During these movements, prey debris and blood were occasionally expelled from the oral cavity, indicating that the behavior caused significant prey disintegration. After a processing bout (i.e., a series of processing cycles), water flows induced by hyobranchial movement transported the food backwards, after which it was either repeatedly processed or swallowed.

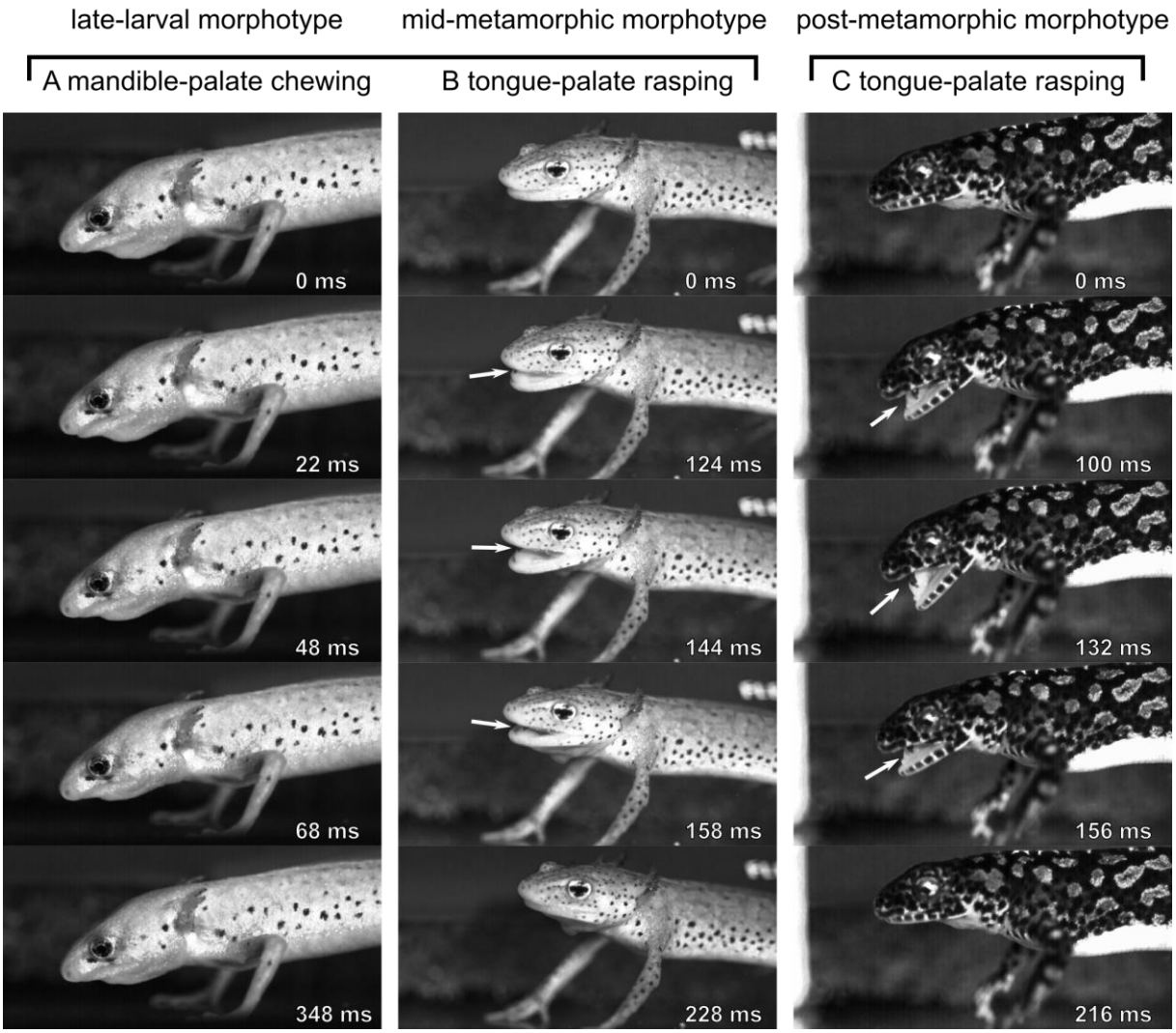

Figure 3 Exemplary snapshots from paedomorphic and metamorphic food processing in *I. alpestris.* **A** mandible-palate chewing in late-larval morphotype (LLM), **B** tongue-palate rasping in mid-metamorphic morphotype (MMM), and **C** tongue-palate rasping in the post-metamorphic morphotype (PMM). Note the similar prey processing patterns of mid-metamorphic morphotype and the post-metamorphic morphotype versus the distinct pattern of late-larval morphotype. The arrows point to the position of the prey item when it is visible from the outside.

Kinematics of intraoral food processing

Intraoral food processing cycles were clearly distinguishable from food transport in that hyobranchial elevation accompanied gape opening during processing, whereas during transport hyobranchial depression accompanied gape opening. During processing, at the onset of gape opening, the LLM initiated hyobranchial elevation, which continued past peak gape opening and reached its peak coincident with complete gape closure. Then, in a returning motion, the hyobranchial apparatus was depressed while the mouth remained shut (i.e., stationary phase). The MMM started elevating the hyobranchial apparatus at the onset of gape opening. Both movements peaked approximately at the same time, after which simultaneous gape closing and hyobranchial depression (i.e., resetting movements) occurred (Fig. 4 B and H). Neither the LLM nor the MMM had stereotypic cranial movements, as indicated by their relative featureless cranial kinematic profiles (Fig. 4 D, E). In the PMM gape and vertical cranial flexion peaks were approximately coincident; thus, gape opening and cranial ventroflexion (or head depression) as well as gape closing and cranial dorsoflexion were aligned (Fig. 4 C and F). The vertical hyobranchial movement had a ~10% phase shift (i.e., delay) from the gape cycle as hyobranchial elevation started at ~90% of the preceding gape cycle (compare Fig. 4 C and I).

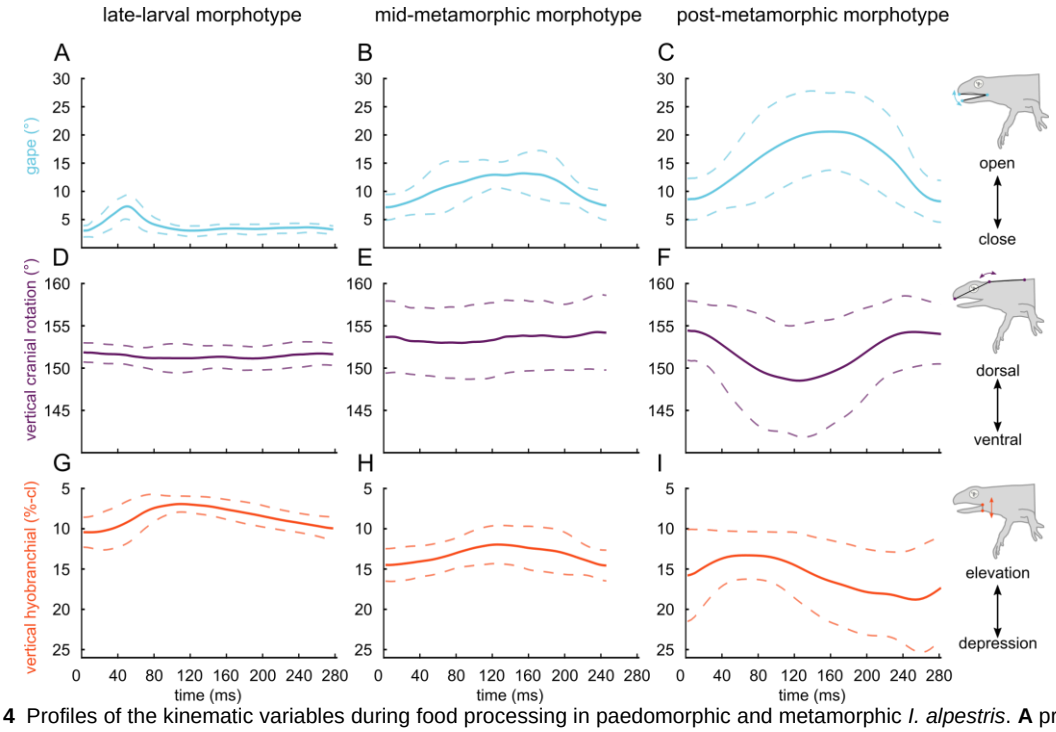

Figure 4 Profiles of the kinematic variables during food processing in paedomorphic and metamorphic *I. alpestris*. **A** processing profile from 18 cycles of the late-larval morphotype (LLM), **B** processing profile from 27 cycles of the mid-metamorphic morphotype (MMM), **C** processing profile from 105 cycles from the post-metamorphic morphotype (PMM). Kinematic means (dark and bold profiles) ± SD (slender, dashed and pale curves) of synchronous motions plotted in normalized coordinate systems with group-normalized timescales (x-axes) for comparison. Gape (light blue) (Fig. 4 A, B, C) and cranial flexion (purple) (Fig. 4 D, E, F) in degree, vertical hyobranchial movement (orange) (Fig. 4 G, H, I) normalized to cranial length (i.e., %-cl).

Table 1 shows the kinematic parameters of food processing in the three morphotypes. The stationary gape phase in the LLM clearly differed from the other two morphotypes (compare Fig. 4A with B and C) as did the cranial flexion of the PMM (compare Fig. 4F with D and E).

Table 1: Kinematic parameters of intraoral food processing in *I. alpestris*

Kinematic variable	Kinematic parameter	Late-larval morphotype (LLM)		Mid-metamorphic morphotype (MMM)		Post-metamorphic morphotype (PMM)	
		Mean ± S.D.	C_V	Mean ± S.D.	C_V	Mean ± S.D.	C_V
Gape	1 Opening (°)	5.35±1.54	0.29	9.82±4.28	0.44	19.30±5.90	0.24
	2 Closure (°)	5.51±1.21	0.22	9.48±4.68	0.49	19.66±5.86	0.23
	3 Opening duration (s)	0.04±0.02	0.45	0.13±0.06	0.48	0.16±0.06	0.32
	4 Closure duration (s)	0.06±0.02	0.36	0.11±0.04	0.38	0.12±0.06	0.44
	5 Closure acceleration (deg/s²)	21407±6149	0.29	12253±6989	0.57	18753±10472	0.45
	6 Open-close duration (s)	0.10±0.03	0.25	0.24±0.07	0.27	0.28±0.07	0.21
	7 stationary duration (s)	0.17±0.08	0.45	n/a	n/a	n/a	n/a
	8 Cycle duration (s)	0.28±0.09	0.33	0.24±0.07	0.27	0.28±0.07	0.21
Vertical cranial flexion	9 Ventral (°)	n/a	n/a	n/a	n/a	12.61±6.51	0.39
	10 Dorsal (°)	n/a	n/a	n/a	n/a	12.30±6.46	0.40
	11 Ventral duration (s)	n/a	n/a	n/a	n/a	0.10±0.05	0.41
	12 Dorsal duration (s)	n/a	n/a	n/a	n/a	0.17±0.07	0.33
	13 Cycle duration (s)	n/a	n/a	n/a	n/a	0.28±0.07	0.21
Vertical hyobranchial movement	14 Elevation (%-cl)	4.29±1.99	0.46	4.93±1.47	0.30	10.57±6.18	0.53
	15 Depression (%-cl)	3.87±1.34	0.35	5.43±1.50	0.28	12.46±5.64	0.36
	16 Elevation duration (s)	0.08±0.02	0.24	0.14±0.06	0.45	0.13±0.05	0.34
	17 Depression duration (s)	0.20±0.09	0.44	0.10±0.03	0.35	0.14±0.05	0.31
	18 Cycle duration (s)	0.28±0.10	0.35	0.23±0.07	0.28	0.27±0.07	0.23

Abbreviations: S.D. standard deviation, C_V coefficient of variation and n/a not applicable. Note that parameters 5 and 7 are identical for both MMM and the PMM. This is because both MMM and PMM lack a stationary phase during processing (parameter 6), so that opening and closing the mouth corresponds to the gape cycle. Note the stereotypy of the magnitude of gape movements (parameter 1 and 2) in the LLM, the flexibility of the gape movements (parameter 1-4) in the MMM, the stereotypy of the hyobranchial movements (parameter 13,14, and 17) in the MMM, the stereotypy of the gape movements (parameter 1,2,3, and 5) in the PMM, and the flexibility of hyobranchial movements (parameter 13-15) in the PMM.

Table 2: Statistics analysis of intraoral food processing kinematics in *I. alpestris*

Kinematic variable	Kinematic parameter	All Morphotypes		LLM vs. MMM		LLM vs. PMM		MMM vs. PMM	
		Kruskal-Wallis H	*p*-value	Mann-Whitney U	*p*-value	Mann-Whitney U	*p*-value	Mann-Whitney U	*p*-value
Gape	Opening	78.08	0.00*	-21.42	0.32	-80.09	0.00*	-58.67	0.00*
	Closure	79.09	0.00*	-17.58	0.55	-78.61	0.00*	-61.03	0.00*
	Opening duration	44.82	0.00*	-57.24	0.00*	-73.85	0.00*	-16.61	0.23
	Closure duration	30.18	0.00*	60.29	0.00*	59.85	0.00*	-0.43	1.00
	Closure acceleration	17.15	0.00*	51.24	0.00*	22.12	0.12	-29.12	0.00*
	Open-close duration	48.69	0.00*	-61.43	0.00*	-77.14	0.00*	-15.72	0.28
	Cycle duration	3.56	1.00	n/a	n/a	n/a	n/a	n/a	n/a
Vertical hyobranchial movement	Elevation	32.10	0.00*	-10.04	1.00	-49.48	0.00*	-39.45	0.00*
	Depression	64.27	0.00*	-18.06	0.52	-71.98	0.00*	-53.92	0.00*
	Elevation duration	18.37	0.00*	-49.55	0.00*	-45.79	0.00*	3.76	1.00
	Depression duration	33.78	0.00*	70.21	0.00*	23.89	0.09	-46.32	0.00*
	Cycle duration	5.22	0.88	n/a	n/a	n/a	n/a	n/a	n/a

Statistical analysis was calculated using Kruskal-Wallis 1-way ANOVA and only performed on parameters present in all morphotypes. *P*-values were Bonferroni adjusted to account for multiple testing; significant *p*-values are indicated by asterisks.

Some significant changes concern the duplication of the vertical hyobranchial magnitude of the PMM compared to the MMM (compare with Fig. 4H and I), the duplication in gape magnitude from the MMM to PMM (compare Fig. 4B and C), and the significantly higher mean mandible acceleration from peak gape opening to reaching maximal gape-closing speed in the LLM compared to the MMM. The durations of the gape and vertical hyobranchial movement cycle are the same across all morphotypes.

Ordination analysis of processing kinematics

A principal component analysis (PCA) was performed to analyze how the processing kinematics of the three morphotypes relate to each other and to visualize differences. Distribution of the chewing cycles among the processing modes and morphotypes on the first two principal components axes Figure 5, and the loadings of the kinematic parameters on principal component 1 and 2 (i.e., PC1 and PC2) are given in Table 3. Hyobranchial kinematics load more strongly on PC1 while mandible kinematics loaded more strongly on PC2. Processing in PMM and LLM are separated in kinematic space with no overlap, but MMM processing overlaps with both LLM and PMM.

The coefficient of variation (C_V) was calculated for each kinematic parameter (Table 1) in order to quantify the stereotypy of the processing behavior of each morphotype [54]. The stationary gape phase (i.e., parameter 6) was only part of the processing mechanism in the LLM and parameters concerning vertical cranial flexion (8-12) could only be analyzed for the PMM. Consequently, these parameters were excluded for comparison.

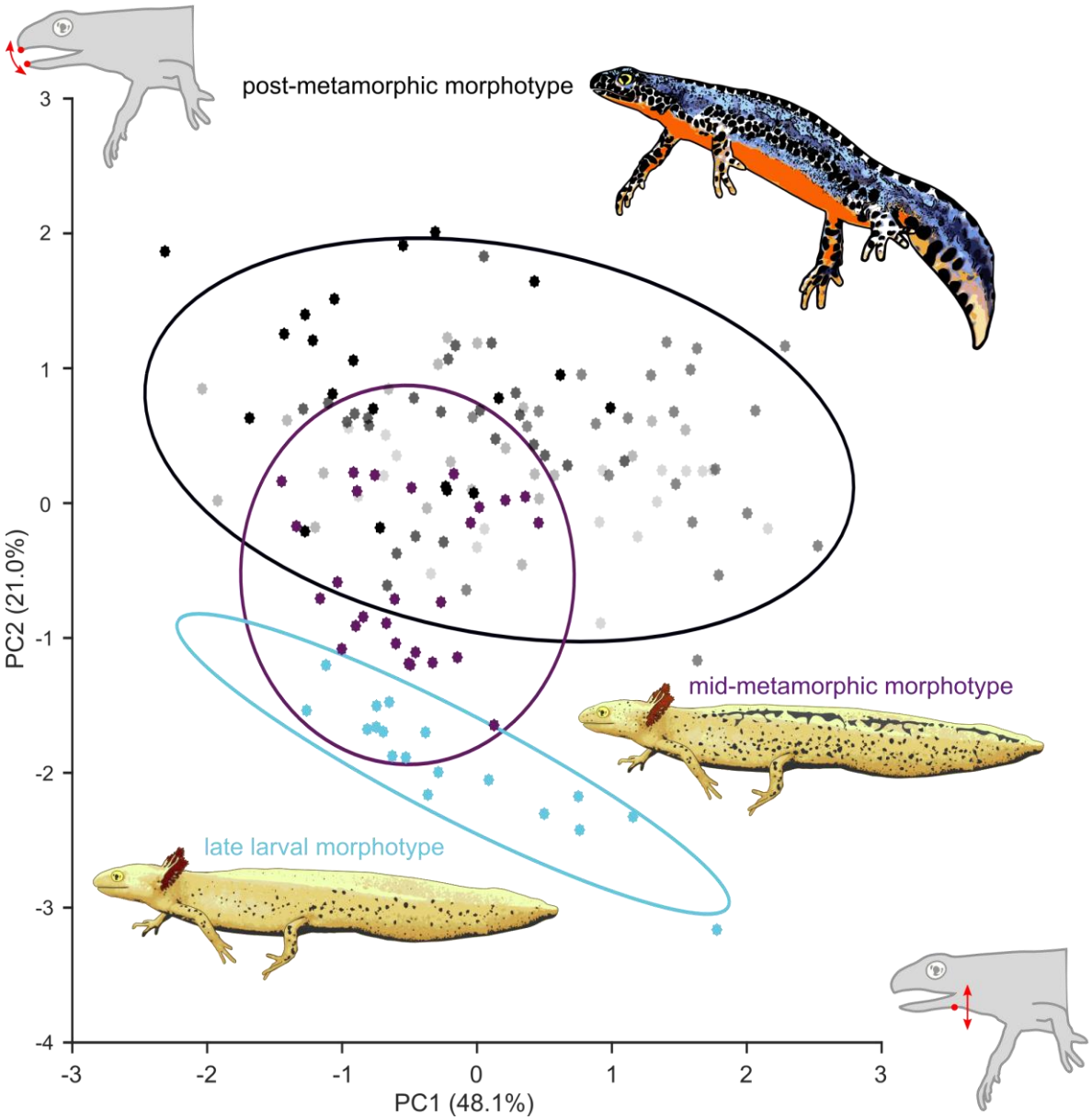

Figure 5 Scatterplots of the first two principal components. The principal components (PC1 and PC2) derived from 5 of 11 kinematic parameters and illustrate differences between the three processing modes in kinematic space. Light blue, processing in the late-larval morphotype (LLM); purple, processing in the mid-metamorphic morphotype (MMM); and black, processing in post-metamorphic morphotypes (PMM) (5 shades of grey code the post-metamorphic individuals). The ellipses display 95 %

confidence interval of the respective feeding mode. PC1 explains 48.1% of the total variance and is mostly defined by hyobranchial parameters, while PC2 explains 21.0% of the total variance and is most strongly defined by gape parameters (Table 3). Note that while LLM and MMM on the one hand and MMM and PMM on the other hand show overlaps, LLM and PMM show no overlap in kinematic space.

Table 3: Loadings of processing parameters on the first two principal components (PC1 and PC2)

Parameter	PC1	PC2
(18) Duration hyobranchial movement cycle	0.836*	-0.123
(15) Magnitude hyobranchial depression	0.779*	0.353
(14) Magnitude hyobranchial elevation	0.663*	0.480
(1) Magnitude gape opening	-0.036	0.872*
(3) Duration gape opening	0.300	0.699*
Total variance explained (%)	48.1	21.0

Parameters marked with * load strongly (> 0.5) on each respective principal component. Note that parameters connected to hyobranchial movement load more strongly in PC1 while parameters connected to gape movements load more strongly on PC2.

Stomach content analysis

Post-metamorphic newts used in stomach content analysis applied suction feeding to ingest lake fly larvae (*Chironomidae*). After ingestion, the newts used cyclic processing movements involving ventral cranial flexion and mouth opening accompanied by hyolingual elevation. Microscopic examinations of the processed lake fly larvae extracted from the stomachs of freshly euthanized newt specimens revealed clear lesions and other structural damage. Lesions were recognized by intensified methylene blue staining, which gradually attenuated along the unharmed part of the prey (Fig. 6B - D). By contrast, unprocessed lake fly larvae (control) only showed blue coloration in the posterior most region (Fig. 6A) and no structural damage. From a total of 100 processed lake fly larvae, 61 exhibited minor to major structural damage (see figure 6B - C), 18 were ruptured (see figure 1 D) and 21 did not show evidence of damage (Fig. 6A).

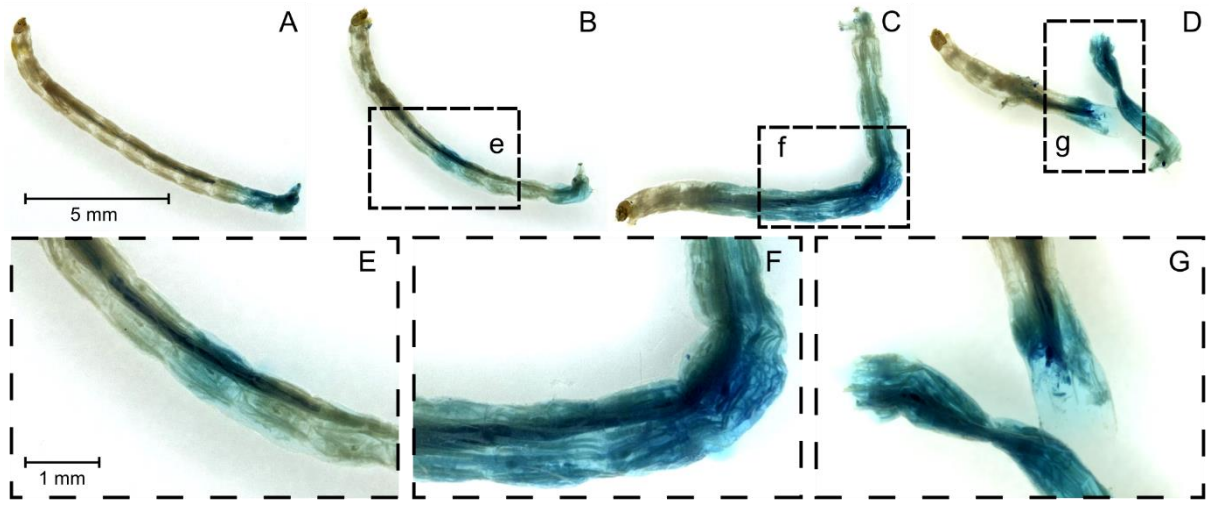

Figure 6: Lake fly larvae (*Chironomidae*) after intraoral processing. (A) Control specimen, and (B-C) processed larvae. The processed specimen exhibited (B) minor injuries, (C) major injuries, and (D) ruptures. Methylene blue staining highlight structural damages in the cuticle. The images E-G show details of the image sections e-g. Note that all samples (including the control) have a blue colored posterior area, probably due to the anal opening.

Discussion

We found distinct intraoral food processing kinematics (Fig. 5) and feeding apparatus morphologies (Fig. 1 and 2) in the three heterochronic morphotypes of the Alpine newt. Thus, this study

shows that externally similar animals can have different internal anatomies, which in turn may result in different food processing mechanisms.

It was recently shown that metamorphosed salamandrid newts use loop-like movements of their hyobranchial apparatus (i.e., tongue) to translate food across the palatal dentition (i.e., tongue-palate rasping) [20]. It has also been suggested that salamandrids with a larval morphology cannot employ the same processing mechanism as metamorphic animals because of morphological constraints, including the lack of a movable tongue and diverging dentition patterns in larval morphotypes [14,15]. To address the question of how processing differs between larval and metamorphosed salamanders within the same species, we examined heterochronic morphotypes of adult Alpine newts.

Despite the remarkably different hyobranchial and cranial morphologies in larval and metamorphic salamanders [37], prey capture and transport only differ marginally across those stages [14,17,18]. We hypothesized a stronger ontogenetic effect on processing kinematics compared to capture and transport, because of the observed morphological differences of the hyobranchial apparatus, ranging from relatively rigid with only limited internal movement-potential in late-larval morphotypes (LLM) to relatively flexible with great internal movement-potential in the post-metamorphic morphotype (PMM), as well as distinct mandible morphologies and differing vomerine tooth patterns. Our data support this hypothesis, as we observed many differences in prey processing behavior across heterochronic morphotypes (Table 1 and Fig. 5). First, gape excursion, which consists of gape opening and closure, is lowest in the LLM, mid-range in the MMM, and greatest as well as significantly different from the aforementioned in the PMM (Table 1 and 2). Similarly, the duration of the gape excursion is shortest in the LLM, mid-range in the MMM, and largest in the PMM - whereby that of MMM and PMM differ significantly from that of the LLM (Table 1 and 2). The extent and duration of the gape opening, which are roughly on the order of the extent and duration of the gape closure, loaded most heavily on PC2 (0.872 and 0.699 respectively) - which separates the kinematics of the three processing modes in kinematic space (Fig. 5 and Table 3). Second, the LLM was the only morphotype to exhibit a stationary phase after the gape cycle and the PMM was the only morphotype to show cranial flexion during processing (Fig. 4 and Table 1). Third, movements of the hyobranchial apparatus in the PMM were significantly greater than either in the LMM or MMM (Table 1 and 2). In sum, the MMM differed in 6 out of 12 kinematic parameters from the LLM, the PMM in 8 out of 12 kinematic parameters from the LLM and the PMM differed in 6 out of 12 kinematic parameters from MMM – suggesting that they apply different food processing mechanisms.

The PMM of the Alpine newts used its tongue to cyclically and rhythmically drive the food against the vomerine dentition on the palate (Fig. 3C and Video 3), very similar to movement patterns reported for the crested newt [20], that uses tongue-palate rasping to process prey. In fact, our stomach content analysis revealed that processing in *I. alpestris* caused substantial mechanical damage to the food objects (Fig. 6). Tongue-palate rasping in the PMM was characterized by relatively stereotypical movements of the mandible (C_V between 0.21-0.32, except for the relatively variable gape closure duration and acceleration with 0.44 and 0.45 respectively) and relatively flexible tongue movements (C_V between 0.31-0.53, except for the relatively stereotypical hyobranchial cycle duration with 0.23), which may indicate that the tongue movements need to be flexibly adjusted during processing. Similar to the PMM, the MMM showed evidence of a tongue-palate rasping mechanism being used (Fig. 3 B and

Video 2) with a modified tongue motion pattern (compare Fig. 4B and H to C and I) and small and sporadic cranial movements (Fig. 4E). Tongue-palate rasping in the MMM was characterized by relatively stereotypical movements of the tongue (C_V between 0.28-0.35, excluding the relative flexible duration of hyobranchial elevation with 0.45) and relative flexible mandible movements (C_V between 0.38-0.57, excluding the relative stereotypical gape cycle duration with 0.27). With regard to the switch from chewing to tongue-palate rasping from the LLM to the MMM respectively, this could suggest that a relatively stereotypical motion sequence is used first when mastering a new behavior pattern, while this motion sequence can become more flexible during ontogenesis (as seen in the PMM).

The LLM used a processing mechanism with a restricted amount of gape opening, which prevented us from determining how food was processed. However, we could distinguish the post-ingestion behavior (i.e., jaw and hyobranchial movements) into prey transport (characterized by hyobranchial depression during gape opening [16–18]) and rhythmic food processing (characterized by hyobranchial elevation throughout or during some of the gape opening cycle [20,22]). Food-processing kinematics in the LLM involved the highest mean gape-closure acceleration (Fig. 4A – C and Table 1). As the mandibles of all morphotypes are of approximately the same size and therefore likely have approximately the same mass, the finding that the LLM showed the highest mean gape-closure acceleration, might suggest that they exhibit the highest bite force. This, in turn, could indicate that the dentition of the mandible could be directly involved in intraoral food processing (i.e. chewing). We use the term bite force to describe the result of the action of the mandible elevator muscles modified by the craniomandibular biomechanics [55] and thus the force that the mandible can transmit onto an object in the oral cavity (therefore not merely equivalent to adductor muscle force). Additionally, one of the most striking characteristics of the LMM cranio-mandibular anatomy is its overbite, causing dentition on the mandible to occlude between the two functional upper jaw systems, creating an effective shearing bite against the palate (Fig. 1 B and C). Consequently, the morphology of the LLM supports the idea that it chews its food using the tooth-bearing mandible (Fig. 1) to pierce the prey against the palate (i.e., ‘mandible-palate clenching’) while the tongue and dentition on both functional upper jaws hold the prey in place. The kinematic profiles support this assumption as initial gape opening is followed by hyobranchial elevation, which potentially act to position and hold the prey in the area of the occlusal surface on the palate, before the mandible accelerates towards the palate (Fig. 4A and G) to bite the prey. Additionally, since the prey occasionally protruded far out of the mouth in the LLM, we were able to observe how the jaws acted on it in a clenching manner (Video 1).

Externally, the processing behavior of LLM showed striking similarities with the chewing behavior of another paedomorphic salamander, *Siren intermedia*. It was shown using high-speed x-ray analyses that *S. intermedia* use its mandible to rasp the prey across the dentition of the palate [22]. Larval Alpine newts, however, chew their food using simple arcuate movements of the mandible (i.e. opening-closing), and switch from chewing to tongue-palate rasping during ontogeny. Tongue-palate rasping appears to become the main food processing mechanism before the tongue is completely remodeled during metamorphosis (Fig. 2 B, 3 B, and Video 2). The behavioral shift from mandible-palate interactions (i.e., chewing) to tongue-palate rasping corresponds with the key morphological changes between morphotypes. Whereas in the LLM the teeth of the V-shaped mandible impinge on the palate between the dentition of both functional upper jaw systems, the U-shaped mandible of the MMM and

the PMM would occlude with more lateral elements of the primary upper jaw (i.e., maxilla) (Fig. 1F-G and 1J-K) upon jaw closing. The change in mandible shape might prevent mandible-based processing in a progressed metamorphic morphotype as (i) there is only a limited occlusal surface between the mandible and primary upper jaw for chewing and (ii) food loading might be insufficient, given that there is no bone bridge between the rear end of the primary maxilla and the anterior quadrato-squamosal region [56]. Food processing is often argued as being important for the immobilization and break-down of food items before swallowing [57–60] so salamanders might need alternative food processing mechanisms once their mandible outgrows its chewing function. Interestingly, this flexible switch from one processing mechanism to another took place in a single stage of development. Both morphotypes (LLM and MMM) were neotenic. This appears to reflect the complex morphological life cycle of many salamanders, in which there may be different morphological expressions of neoteny, with the morphology of some neotenic animals being very similar to that of adults [29]. Not least for this reason, we suspect that the sequence of behaviors we observed could be typical of the development of many salamanders.

It has been previously hypothesized that salamanders show a phylogenetic trend of evolving tongues with greater protrusion potential, increased freedom of the branchial arch in relation to the hyoid arch and that tongue prehension might have evolved from a manipulative function [27]. In line with that idea, we found a concurrent ontogenetic process of remodeling in the tongue apparatus. In which the tongue develops from a bulky relatively inert system (i.e., hyobranchial system) with small protrusion ability in the LLM (Fig. 1D and 2A) to a delicate and relatively mobile system (i.e., hyolingual system) with greater protrusion ability in the PMM (Fig. 1L and 2C). The LLM hyobranchial system has a muscular anatomy that creates motion-potential in all directions of the median plane. However, tongue protraction is limited to geniohyoideus and hyomandibularis which act as the primary tongue protractor complex in larval salamanders (Fig. 2A). During the metamorphosis in the MMM, the branchiohyoideus externus and subarcualis rectus 1 are rearranged to functionally suspend the branchial arch on the paired ceratohyal (i.e., hyoid arch) (Fig. 2B). This muscle rearrangement enables a more effective protraction of the branchial arch, since it can now be moved by the suspension on the hyoid arch and thus pulled further anteriorly (Fig. 2B). This secondary tongue protractor complex allows the tip of the tongue to be ejected out of the mouth which has been described for post-metamorphic salamandrids [32] and in turn is the functional basis for tongue-palate rasping [20]. Our data suggest that aquatic salamandrid larvae begin to use their tongue for processing (Fig. 3B and Video 2) as soon as the mandibular reorganization prevents them from chewing but their tongue morphology enables improved protraction during development. Thus, we hypothesize that salamanders that are able to protract their tongue effectively and have a metamorphic palatal dentition are potentially able to combine these elements to achieve tongue-palate rasping. Consequently, it is likely that tongue-palate rasping is the general processing mechanisms in salamanders with a metamorphic feeding apparatus morphology. Additionally, our data support Regal's hypothesis that tongue prehension likely evolved from a processing or manipulation function of the tongue [27] as our animals mastered tongue-palate rasping before they were apt to leave the water and thus before they used their protractible tongue to catch prey.

Mid-metamorphic Alpine newts develop the ability to rasp a food item against the palatal dentition and engage in tongue-palate rasping due to rearrangements of the branchiohyoideus externus

and subarcualis rectus 1 muscles during metamorphosis. At the same time mid-metamorphic morphotypes also retain the ability to forcefully elevate their tongue using the levator hyoideus muscle (Fig. 2 B). The tongue of the post-metamorphic morphotype loses this muscular connection to the skull (i.e., levator hyoideus) and its motion is limited to elevation based on muscles spanning the mouth floor and the hyobranchial system laterally [34]. As a result, the tongue is likely to lose the ability to forcefully press a food against the palatal dentition, possibly reducing the effectiveness of tongue-palate rasping. It had been hypothesized that the coordination between hyolingual motion and depression of the skull may aid food processing efficacy in metamorphic salamandrids [20]. Coordinated head and hyolingual movement patterns also appear in post-metamorphic Alpine newts (Fig. 4F, I), but not in the mid-metamorphic stage, suggesting that coordinated depression of the skull and hyolingual movements might be a compensatory behavior for the loss of the levator hyoideus (Fig. 2C).

From an evolutionary perspective the findings presented here might shed light on the fish-tetrapod transition (water-land transition) of early tetrapods. While tongue and jaw kinematics are similar across amniotes [23,24,61], food processing in salamanders shares traits with both fish and amniotes [20]. Accordingly, salamanders may be a good analog model to reveal functional changes in feeding behavior across the fish-tetrapod transition [40]. From this point of view, the morphological and behavioral differences between the two aquatic larval stages (LLM and MMM) could reflect analogous changes in the early tetrapods. In particular, the present study shows that the MMM – a stage with both larval and post-metamorphic traits and without a freely movable tongue - utilizes a new feeding mechanism (tongue-palate rasping) before the presumed morphological adjustments for this function have fully developed and while the animal remains fully aquatic. It is possible that behavioral changes may have preceded obvious morphological evolution of the feeding system across the fish-tetrapod transition, resulting in new feeding mechanisms. Thus, understanding the timing of changes in feeding mechanism across the transition may require precise quantification and characterization of morphology as well as rigorous biomechanical testing, which can reveal biomechanical differences in similarly-shaped structures [62]. Furthermore, our results support findings from previous studies that morphological and behavioral changes facilitated the evolution of “terrestrial style feeding” in early tetrapod taxa that were still primarily aquatic [63–66] and thus terrestrial feeding likely evolved in stages across the transition from water to land.

Conclusions

We found differences in the skeleton, soft tissue and food processing kinematics between the LLM and MMM, suggesting previously unappreciated diversity between superficially similar paedomorphic stages. Further, our data show that prey processing kinematics differ between all heterochronic morphotypes in the Alpine newt, contrary to the previously established pattern of stereotypy of prey capture or intraoral transport kinematics for this species. Our data indicate a degree of plasticity not previously demonstrated in the ontogeny of intraoral food processing behaviors. Based on a similar development in the feeding apparatus morphologies of most larval salamanders, our data also suggest that salamanders may undergo similar food processing ontogenies in general. Additionally, we found, that salamanders that are able to protract their tongue effectively and have proper palatal dentition, are potentially equipped to use tongue-palate rasping. Consequently, it is likely that tongue-

palate rasping is a generalized pattern in salamanders with a metamorphic feeding apparatus morphology. Finally, the present study might allow some parallels to be drawn about the evolution of terrestrial feeding in early tetrapods. In analogy to salamanders, early tetrapods might have evolved new feeding mechanisms in their aquatic environments and these functional innovations later might have paved the way for terrestrial feeding mechanisms.

Methods

Specimens and animal care

The paedomorphic and metamorphic specimens used in this study were collected in September of 2012 from an artificial irrigation reservoir in the Province of Bolzano (South Tyrol, Italy) under collection permit No. 63.01.05/120963, granted by the local government of the Province of Bolzano. For further information on the pond and the paedomorphic character of the specimens, see [67]. The natural prey spectrum of metamorphic and paedomorphic *Ichthyosaura alpestris* is very broad. In the aquatic habitat, the Alpine newt feeds on insect larvae (e.g. *Chironomidae*), small crustaceans and amphibian eggs or larvae [68,69].

Kinematic analyses were conducted using five metamorphic individuals (IaM1, IaM2, IaM3, IaM5 and IaF1; M/F = male/female) and two paedomorphic individuals (IaP1 and IaP2; P = paedomorphic). The SVL of paedomorphic specimens (43 and 45 mm) did not differ significantly from the SVL of metamorphic specimens (44.6 ± 3.4 mm). The animals were group-housed with both paedomorphic newts in one aquarium (60 × 30 × 40 cm; (length × width × depth)) and the metamorphic newts in a larger aquarium (120 × 60 × 40 cm). The animals were kept at 20 ± 2 °C temperature, 12/12 h photoperiod and were exclusively fed with lake fly larvae (*Chironomidae*) a week before the recordings.

High-speed recording and kinematic analysis

The newts were placed in a glass aquarium (30 × 12 × 20 cm) with a water level of approximately 10 cm. Paedomorphic and metamorphic individuals were fed with lake fly larvae (*Chironomidae*). A chessboard pattern was placed in the background of the aquarium to allow calibration of the videos. The test setup was illuminated with reduced heat emission spotlights (VD-7000 LP; Vision Devices GmbH, Metzingen, Germany). A high-speed camera (Photron FASTCAM model 100KC; Photron, Tokyo, Japan) was used to record the feeding events at 500 fps with a 1024 × 512 pixel frame format. Recordings of paedomorphic feeding trials was conducted using a 60 mm macro lens while a 50 mm standard lens was used for metamorphic trials. A total of 49 recordings from paedomorphic and 50 recordings from metamorphic newt feeding were acquired.

Recordings for kinematic analyses were selected according to overall sharpness (focus on the specimen) as well as specimen orientation. Landmark tracking was carried out using Simi Motion 8.0.0.315 software (Simi Reality Motion Systems GmbH, Unterschleißheim, Germany). Three component motions - gape cycle, vertical cranial flexion, and dorso-ventral hyobranchial movement - were analyzed. To do so, we tracked six landmarks: (1) tip of the upper jaw, (2) back of the head, (3) reference point on the back approximately over the shoulder girdle (4) tip of the mandible, (5) corner of the mouth, and (6) point ventral to the corner of the mouth which lowers as the hyobranchial apparatus

is depressed (Fig. 7, A-B). Every fifth frame was used for manual landmark tracking, the missing intermediate time steps were spline interpolated, and the resulting motion graphs were locally smoothed using the built-in functions of the tracking software. Using the smoothing and interpolation functions of the tracking software allowed confirmation of the markers' positions on their specific landmarks. In total, 105 processing cycles of metamorphic newts (21 IaM1, 22 IaM2, 24 IaM3, 20 IaM5 and 18 IaF1) and 45 processing cycles of paedomorphic newts (27 IaP1 and 18 IaP2) were analyzed. We used trigonometry on the 2-D landmark coordinates to calculate the kinematic parameters gape (Fig. 7 C), vertical cranial flexion (Fig. 7 D), and vertical hyobranchial movement (Fig. 7 E). Then we used a custom-written script for MATLAB R2019b (The Mathworks, Inc., Natick, MA, USA) to compute the 18 kinematic parameters out of the kinematic variables. All calculations were performed in Excel (Microsoft Corporation, WA, USA) or using a custom script in MATLAB R2019b.

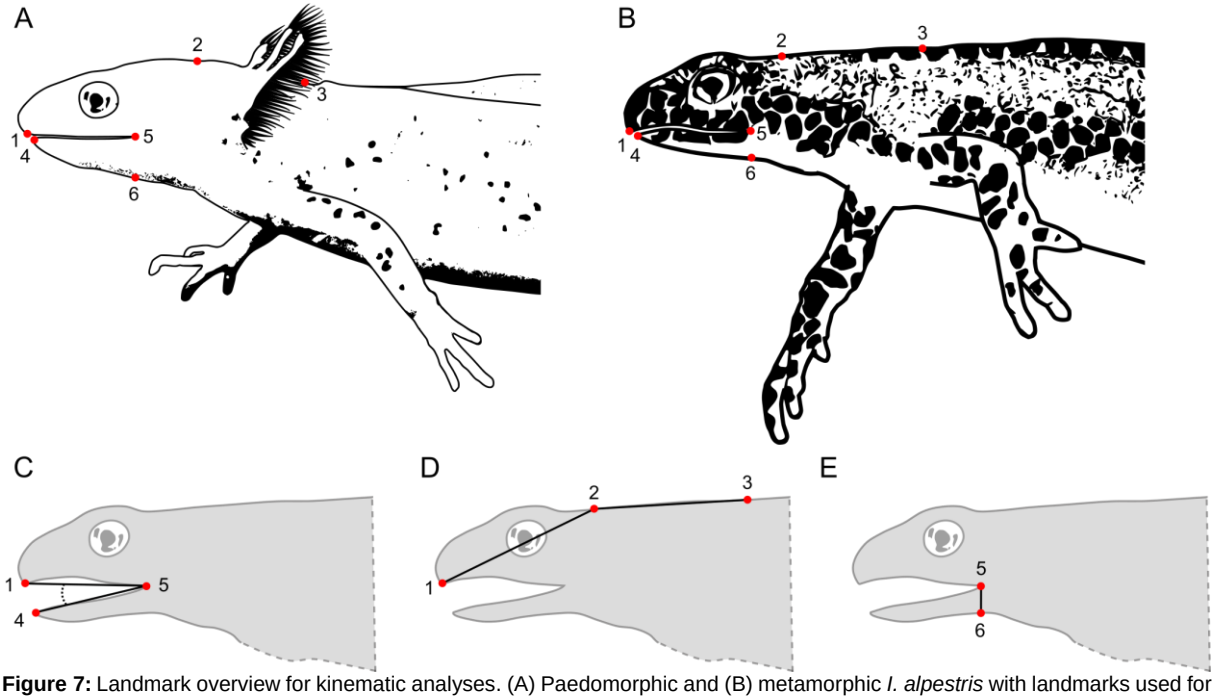

Figure 7: Landmark overview for kinematic analyses. (A) Paedomorphic and (B) metamorphic *I. alpestris* with landmarks used for kinematic analyses. Lower row depicts the calculation of (C) gape, (D) vertical cranial flexion and (E) vertical hyobranchial displacement. Abbreviations: (1) tip of the upper jaw, (2) back of the head, (3) reference point on the back approximately over the shoulder girdle (4) tip of the mandible, (5) corner of the mouth, and (6) point ventral to the corner of the mouth which lowers as the hyobranchium is depressed.

Statistical analysis and ordination approach

The aim of the statistical analysis was to test the kinematic parameters for differences between the morphotypes (LLM, MMM and PMM). Since the parameters violated the assumptions for parametric tests, nonparametric statistics were carried out. To determine if the kinematic parameters differ between morphotypes, we performed a Kruskal-Wallis 1-way ANOVA. The sequential pairwise multiple comparisons (i.e. Mann-Whitney U tests), using ranks based on considering all samples, not just the two samples that are currently involved in a comparison [70], were performed to determine where the differences are among the morphotypes. All significance values were Bonferroni adjusted to account for multiple testing.

The aim of the ordination approach was to visualize how the processing kinematics of the three morphotypes are related and thus by implication to highlight their differences. Seven dimension reductions were performed prior to the principal component analysis (PCA) to remove processing

parameters (2,4-13, 16-17 of Table 1) which do not load strongly (<0.5) on any of the components. The PCA was performed on the correlation matrix and the resulting Anderson-Rubin factor scores were saved in order to show the effects of (i) individual, (ii) heterochronic state, and (iii) processing mode on the total variance. The factor scores of the PCA were plotted with the related confidence intervals of 95 % using a custom-written script for MATLAB R2019b. The principal component analysis was performed using SPSS 25 (IBM Corporation, Armonk, NY, USA).

Stomach content analysis

Once the feeding trials and the kinematic analysis were performed, we fed the metamorphic animals with lake fly larvae *ad libitum*. They were presented with a multitude of lake fly larvae, which they ingested and processed one to several at a time. After feeding, the animals were anaesthetized and subsequently euthanized by immersion in an aqueous solution of 0.5% MS222, buffered to pH 7.0. The stomachs were removed and voided post-mortem and the stomach contents were fixed in 70 % ethanol for one week. The processed lake fly larvae were stained using methylene blue (1 minute) and then washed with 70% ethanol. The processing injuries were recorded using a digital microscope (Keyence, VHX-2000; Keyence Corporation, Osaka, Japan). The paedomorphic specimens died prior to completion of data acquisition; thus, no paedomorphic stomach contents could be analyzed.

Anatomical analysis (µCT)

The musculoskeletal components of the feeding apparatus of paedomorphic and metamorphic specimens were reconstructed from µCT scans [14]. Euthanized specimens were fixed in 4 % formaldehyde for one month, dehydrated in a graded series of ethanol, immersed for two weeks in an alcoholic iodine solution, rinsed in absolute ethanol and securely mounted in Falcon tubes to avoid motion artifacts in the scans. Scans of the entire paedomorphic specimens were acquired using a µCT scanner (SkyScan 2211; Bruker, Billerica, MA, USA) with a source voltage of 100 kV, an electric current of 180 µA, a 0.5 mm Titan filter, and an isometric voxel resolution of 8.00 µm. X-ray projections were then reconstructed in NRecon Reconstruction Software 1.7.3.1 (Micro Photonics, Allentown, PA) with an automatic beam hardening correction factor of 45%. For the metamorphic specimen only scans of the head region were acquired using a µCT scanner (SkyScan 1174) with a source voltage of 50 kV, an electric current of114 µA, a 0.5 mm aluminum filter, and an isometric voxel resolution of 7.39 µm. X-ray projections were also reconstructed in NRecon Reconstruction Software. Volume rendering of the µCT scans was performed using the Amira 6.4 software package (https://www.fei.com/software/amira). Based on tomographic image data, we threshold-segmented bones and used manual segmentation for muscles, cartilage and teeth. Both paedomorphic specimens are kept in the State Museum of Natural History Stuttgart (SMNS 16344 and SMNS 16345).

Competing interests

The authors declare that they have no competing interests.

Availability of data and material

The datasets during and/or analyzed during the current study available from the corresponding author on reasonable request.

Consent for publication

Not applicable

Ethics approval and consent to participate

Experiments were performed at the Friedrich-Schiller-University of Jena, Germany. The Committee for Animal Research of the State of Thuringia, Germany, approved husbandry and experiments (codes animal experiments: 02-042/14, 02-008/15; code animal husbandry: J-SHK-2684-05-04-05-07/14).

Acknowledgements

We thank Julia Grell for her help with high-speed recordings of paedomorphic newts, Stephan Handschuh (University of Veterinary Medicine Vienna) for conducting the µCT-scans of the metamorphic specimens, Manuel Hopf for coding of our MATLAB scripts, and Alexander Stößel for conducting the µCT-scans of the paedomorphic specimens.

Funding

This study was funded by the Deutsche Forschungsgemeinschaft (DFG grant 7788/1-1 to E.H.) and by University of Massachusetts Lowell (start-up funds to N.K).

Authors' contributions

DS and EH designed the study. EH, LBP, and NK oversaw the experimental design. DS collected data (high-speed experiments), designed and performed the data analysis, created the three-dimensional reconstruction, conducted the morphological description, prepared the figures and interpreted the results. DS wrote the first manuscript with help, guidance and review from EH, LBP, and NK.

References

1. Lofts B. Physiology of the Amphibia. Elsevier; 2012.
2. Hanken J. Chapter 3 – Larvae in Amphibian Development and Evolution. Orig Evol Larval Forms. 1999. p. 61–108.
3. Vitt LJ, Caldwell JP. Chapter 2 – Anatomy of Amphibians and Reptiles. Herpetology. Fourth. 2014. p. 35–82.
4. Pierce BA, Smith HM. Neoteny or Paedogenesis? J Herpetol. 1979;13:119–21.
5. Semlitsch RD. Paedomorphosis in *Ambystoma talpoideum*: Effects of Density, Food, and Pond Drying. Ecology. 1987;68:994–1002.
6. Hayes TB. Hormonal mechanisms as potential constraints on evolution: Examples from the anura. Am Zool. 1997;37:482–90.
7. Gould SJ. Ontogeny and phylogeny. Harvard University Press; 1977.
8. Denoël M, Poncin P. The effect of food on growth and metamorphosis of paedomorphs in *Triturus alpestris apuanus*. Arch fur Hydrobiol. 2001;152:661–70.
9. Wiens JJ, Bonett RM, Chippindale PT. Ontogeny Discombobulates Phylogeny: Paedomorphosis and Higher-Level Salamander Relationships. Syst Biol. 2005;54:91–110.
10. Matsuda R. The evolutionary process in talitrid amphipods and salamanders in changing environments, with a discussion of "genetic assimilation" and some other evolutionary concepts. Can J Zool. 1982;60:733–49.
11. Lauder G V., Shaffer HB. Functional Design of the Feeding Mechanism in Lower-Vertebrates - Unidirectional and Bidirectional Flow Systems in the Tiger Salamander. Zool J Linn Soc. 1986;88:277–90.

12. Reilly S. The ontogeny of aquatic feeding behavior in *Salamandra salamandra*: stereotypy and isometry in feeding kinematics. J Exp Biol. The Company of Biologists Ltd; 1995;198:701–8.
13. Reilly SM, Lauder G V. Ontogeny of aquatic feeding performance in the eastern newt, *Notophthalmus viridescens* (Salamandridae). Copeia. JSTOR; 1988;87–91.
14. Heiss E, Grell J. Same but different: aquatic prey capture in paedomorphic and metamorphic Alpine newts. Zool Lett. Zoological Letters; 2019;5:1–12.
15. Shaffer HB, Lauder G V. The ontogeny of functional design: metamorphosis of feeding behaviour in the tiger salamander (<i>Ambystoma tigrinum). J Zool. Wiley Online Library; 1988;216:437–54.
16. Reilly SM, Lauder G V. Prey transport in the tiger salamander:quantitative electromography and muscle function in tetrapods. J exp Zool. 1991;260:1–17.
17. Gillis GB, Lauder G V. Aquatic Prey Transport and the Comparative Kinematics of *Ambystoma tigrinum* Feeding Behaviors. J Exp Biol [Internet]. 1994;187:159–79. Available from: http://www.ncbi.nlm.nih.gov/pubmed/9317549
18. Reilly SM, Lauder G V. The Evolution of Tetrapod Feeding Behavior: Kinematic Homologies in Prey Transport. Evolution (N Y) [Internet]. 1990;44:1542–57. Available from: http://www.jstor.org/stable/2409336?origin=crossref%5Cnpapers3://publication/doi/10.2307/2409336
19. Reilly SM. The Metamorphosis of Feeding Kinematics in *Salamandra salamandra* and the Evolution of Terrestrial Feeding Behavior. J Exp Biol [Internet]. 1996;199:1219–27. Available from: http://www.ncbi.nlm.nih.gov/pubmed/9319073
20. Heiss E, Schwarz D, Konow N. Chewing or not? Intraoral food processing in a salamandrid newt. J Exp Biol. The Company of Biologists Ltd; 2019;jeb-189886.
21. Schwenk K, Wake DB. Prey processing in *Leurognathus marmoratus* and the evolution of form and function in desmognathine salamanders (Plethodontidae). Biol J Linn Soc. 1993;49:141–62.
22. Schwarz D, Konow N, Roba YT, Heiss E. A salamander that chews using complex, three-dimensional mandible movements. J Exp Biol. The Company of Biologists Ltd; 2020;223.
23. Konow N, Herrel A, Ross CF, Williams SH, German RZ, Sanford CPJ, et al. Evolution of Muscle Activity Patterns Driving Motions of the Jaw and Hyoid during Chewing in Gnathostomes. Integr Comp Biol. 2011;51:235–46.
24. Ross CF, Baden AL, Georgi J, Herrel A, Metzger KA, Reed DA, et al. Chewing variation in lepidosaurs and primates. J Exp Biol [Internet]. 2010;213:572–84. Available from: http://jeb.biologists.org/cgi/doi/10.1242/jeb.036822
25. Greven H, Kamp T Van De, Rolo S, Baumbach T, Clemen G. Vomeropterygopalatina in larval *Ichthyosaura alpestris apuanus* (Amphibia: Urodela) and comments on the formation of the definite vomer in the Salamandridae. Vertebr Zool. 2017;67:179–96.
26. Clemen G, Greven H. Remodelling of the palate: an additional tool to classify larval salamandrids through metamorphosis. Vertebr Zool. 2013;63:207–16.
27. Regal PJ. Feeding Specializations and the Classification of Terrestrial Salamanders. Soc Study Evol. 1966;20:392–407.
28. Clemen G, Greven H. The buccal cavity of larval and metamorphosed *Salamandra salamandra*: Structural and developmental aspects. Mertensiella. 1994;4:9.
29. Reilly SM. Ontogeny of the Hyobranchial apparatus in the salamanders *Ambystoma talpoideum*

(Ambystomatidae) and *Notophthalmus viridescens* (Salamandridae): the ecological morphology. J Morphol [Internet]. 1987;214:205–14. Available from: http://onlinelibrary.wiley.com/doi/10.1002/jmor.1051910210/abstract
30. Djorović A, Kalezić ML. Paedogenesis in European Newts (*Triturus: Salamandridae*): Cranial Morphology During Ontogeny. J Morphol. 2000;243:127–39.
31. Noble GK. Further observations on the life-history of the newt, *Triturus viridescens*. Am Museum Novit. New York City: American Museum of Natural History; 1929;348:1–22.
32. Findeis EK, Bemis WE. Functional morphology of tongue projection in *Taricha torosa* (Urodela: Salamandridae). Zool J Linn Soc. Wiley Online Library; 1990;99:129–57.
33. Heatwole H, Rose CS. The developmental morphology of salamander skulls. Amphib Biol. 2003;5:1684–781.
34. Reilly SM, Lauder G V. Kinetics of tongue projection in *Ambystoma tigrinum*: quantitative kinematics, muscle function, and evolutionary hypotheses. J Morphol. Wiley Online Library; 1989;199:223–43.
35. Reilly SM. Ontogeny of cranial ossification in the eastern newt, *Notophthalmus viridescens* (Caudata: Salamandridae), and its relationship to metamorphosis and neoteny. J Morphol. 1986;188:315–26.
36. Schoch RR, Pogoda P, Kupfer A. The impact of metamorphosis on the cranial osteology of giant salamanders of the genus *Dicamptodon*. Acta Zool. Wiley Online Library; 2019;
37. Ivanović A, Cvijanović M, Denoël M, Slijepčević M, Kalezić ML. Facultative paedomorphosis and the pattern of intra-and interspecific variation in cranial skeleton: lessons from European newts (*Ichthyosaura alpestris* and *Lissotriton vulgaris*). Zoomorphology. Springer; 2014;133:99–109.
38. Ziermann JM, Diogo R. Cranial muscle development in the model organism *Ambystoma mexicanum*: Implications for tetrapod and vertebrate comparative and evolutionary morphology and notes on ontogeny and phylogeny. Anat Rec. 2013;296:1031–48.
39. Lauder G V., Reilly SM. Metamorphosis of the feeding mechanism in tiger salamanders (*Ambystoma tigrinum*): the ontogeny of cranial muscle mass. J Zool Lond. Wiley Online Library; 1990;222:59–74.
40. Lauder G V, Reilly SM. Amphibian Feeding Behavior: Comparative Biomechanics and Evolution. Adv Comp Environ Physiol [Internet]. Springer-Verlag Berlin Heidelberg GmbH; 1994. p. 163–95. Available from: http://link.springer.com/10.1007/978-3-642-57906-6_7%5Cnpapers3://publication/doi/10.1007/978-3-642-57906-6_7
41. Schoch RR. The evolution of metamorphosis in temnospondyls. Lethaia. Wiley Online Library; 2002;35:309–27.
42. Fortuny J, Marcé-Nogué J, De Esteban-Trivigno S, Gil L, Galobart À. Temnospondyli bite club: ecomorphological patterns of the most diverse group of early tetrapods. J Evol Biol. Wiley Online Library; 2011;24:2040–54.
43. Schoch RR. Evolution of life cycles in early amphibians. Annu Rev Earth Planet Sci. Annual Reviews; 2009;37:135–62.
44. Witzmann F. Phylogenetic patterns of character evolution in the hyobranchial apparatus of early tetrapods. 2013;145–67.
45. Özeti N, Wake DB. The morphology and evolution of the tongue and associated structures in salamanders and newts (family *Salamandridae*). Am Soc Ichthyol Herpetol. JSTOR; 1969;1969:91–123.

664 46. Heiss E, Handschuh S, Aerts P, Van Wassenbergh S. Musculoskeletal architecture of the prey
665 capture apparatus in salamandrid newts with multiphasic lifestyle: does anatomy change during the
666 seasonal habitat switches? J Anat. Wiley Online Library; 2016;228:757–70.
667 47. Bauer WJ. A contribution to the morphology of visceral jaw-opening muscles of urodeles (Amphibia:
668 Caudata). J Morphol. Wiley Online Library; 1997;233:77–97.
669 48. Smith GM. The detailed anatomy of *Triturus torosus*. University of British Columbia; 1926.
670 49. Marconi M, Simonetta AM. The Morphology of the Skull in Neotenic and normal *Triturus vulgaris*
671 *meridionale* (Boulenger)(Amphibia Caudata Salamandridae). Monit Zool Ital J Zool. Taylor & Francis;
672 1988;22:365–96.
673 50. Tarapani H. Zur Entwicklungsgeschichte des Hyobranchialskelettes von *Salamandra atra* Laur. und
674 *Triton alpestris* Laur. [Zürich]: Gustav Fischer Jena; 1909.
675 51. Heiss E, Handschuh S, Aerts P, Van Wassenbergh S. A tongue for all seasons: extreme phenotypic
676 flexibility in salamandrid newts. Sci Rep. Nature Publishing Group; 2017;7:1–10.
677 52. Kleinteich T, Herzen J, Beckmann F, Matsui M, Haas A. Anatomy, Function, and Evolution of Jaw
678 and Hyobranchial Muscles in Cryptobranchoid Salamander Larvae. J Morphol. 2014;275:230–46.
679 53. Ziermann JM. Diversity of Heads, Jaws, and Cephalic Muscles in Amphibians. Heads, Jaws, and
680 Muscles. Springer; 2019. p. 143–70.
681 54. Wainwright PC, Mehta RS, Higham TE. Stereotypy, flexibility and coordination: key concepts in
682 behavioral functional morphology. J Exp Biol [Internet]. 2008;211:3523–8. Available from:
683 http://jeb.biologists.org/cgi/doi/10.1242/jeb.007187
684 55. Koc D, Dogan A, Bek B. Bite force and influential factors on bite force measurements: a literature
685 review. Eur J Dent. Thieme Medical and Scientific Publishers Private Ltd.; 2010;4:223–32.
686 56. Fortuny J, Marce-Nogue J, Heiss E, Sanchez M, Gil L, Galobart À. 3D bite modeling and feeding
687 mechanics of the largest living amphibian, the Chinese giant salamander *Andrias davidianus* (Amphibia:
688 Urodela). PLoS One. Public Library of Science; 2015;10.
689 57. Throckmorton GS. Oral food processing in two herbivorous lizards, *Iguana iguana* (Iguanidae) and
690 *Uromastix aegyptius* (Agarnidae). J Morphol. 1976;148:363–90.
691 58. Schwenk K. Chapter 2 – An Introduction to Tetrapod Feeding. Feeding. 2000;21–61.
692 59. Reilly SM, McBrayer LD, White TD. Prey processing in amniotes: Biomechanical and behavioral
693 patterns of food reduction. Comp Biochem Physiol - A Mol Integr Physiol. Elsevier; 2001;128:397–415.
694 60. Lucas PW, Luke DA. Chewing it over: basic principles of food breakdown. Food Acquis Process
695 primates. Springer; 1984. p. 283–301.
696 61. Gintof C, Konow N, Ross CF, Sanford CPJ. Rhythmic chewing with oral jaws in teleost fishes: a
697 comparison with amniotes. J Exp Biol [Internet]. 2010;213:1868–75. Available from:
698 http://jeb.biologists.org/cgi/doi/10.1242/jeb.041012
699 62. Lautenschlager S, Brassey CA, Button DJ, Barrett PM. Decoupled form and function in disparate
700 herbivorous dinosaur clades. Sci Rep. Nature Publishing Group; 2016;6:26495.
701 63. Ahlberg PE, Clack JA, Blom H. The axial skeleton of the Devonian tetrapod Ichthyostega.
702 2005;437:137–40.
703 64. Clack JA. Gaining ground: the origin and evolution of tetrapods. Indiana University Press; 2012.
704 65. Markey MJ, Marshall CR. Terrestrial-style feeding in a very early aquatic tetrapod is supported by

evidence from experimental analysis of suture morphology. Proc Natl Acad Sci U S A. 2007;104:7134–8.

66. Porro LB, Rayfield EJ, Clack JA. Descriptive anatomy and three-dimensional reconstruction of the skull of the early tetrapod Acanthostega gunnari Jarvik, 1952. PLoS One. Public Library of Science; 2015;10.

67. Heiss E. The Alpine “axolotl”: a remarkable example of phenotypic plasticity in *Ichthyosaura alpestris* (Amphibia : Salamandridae). Salamandra. 2017;53:137–41.

68. Sattmann H. Über die Nahrung des Bergmolches, *Triturus alpestris* (LAURENTI, 1768), in der aquatischen Phase (Caudata: Salamandridae). Herpetozoa. 1989;2:37–49.

69. Denoël M, Andreone F. Trophic habits and aquatic microhabitat use in gilled immature, paedomorphic and metamorphic Alpine newts (*Triturus alpestris apuanus*) in a pond in central Italy. Belgian J Zool. Société royale zoologique de Belgique; 2003;133:95–102.

70. Dunn OJ. Multiple comparisons using rank sums. Technometrics. Taylor & Francis Group; 1964;6:241–52.